JOURNAL OF APPLIED ELECTROCHEMISTRY 22 (1992) 801–809

Dynamic analysis of charge transport in fluidized bed electrodes: impedance techniques for electro-inactive beds

C. GABRIELLI, F. HUET, A. SAHAR

LP15 du CNRS, Physique des Liquides et Electrochimie, Laboratoire de l'Université Pierre et Marie Curie, Tour 22, 4 place Jussieu, 75252 Paris Cedex 05, France

G. VALENTIN

Laboratoire des Sciences du Génie Chimique, ENSIC, Nancy, France

Received 30 August 1990; accepted 9 February 1992

A model of charge transport in fluidized bed electrodes, based on the model of Newman and Tobias, is proposed. It explains the dynamic behaviour of these particulate electrodes in terms of a.c. impedance thanks to a description based on a transmission line. In the case of gold beads in 1 M NaOH solution, the impedance related to the mean contact between the particles, the interfacial impedance of the particle–solution and the solution resistivity can be obtained.

1. Introduction

In electrolysers of practical interest, the active area per unit volume of electrode is a parameter of great importance. The fluidized bed electrolyser has been proposed to optimize this parameter as described through two patents [1, 2] in 1966. To date, little commercial use of this electrolyser has been made. A few applications can be found for fuel cells, organic electrosynthesis, precious metal electrowinning from very dilute solutions, non-precious metal mining and batteries. If the working conditions of the electrolyser are not well chosen it consumes more energy than a conventional electrolysis cell. This may be due, when high current densities are used in the counter electrode chamber: (i) to a greater resistance to current flow related to the intermittent contact between the conducting particles and (ii) to concomitant potential distributions in the bulk of the fluidized bed which lead to parasitic gas evolution or incomplete use of the whole active surface. Therefore, the use of the fluidized bed electrolyser has hitherto been limited because its electrical and electrochemical behaviour are insufficiently understood [3–11].

A fluidized bed electrode consists of solid metallized or metallic particles dispersed by an upward flow of a fluid. The fluid is injected through a perforated distributor, through a calming section which imposes a uniform fluid velocity over the whole cross-section of the bed. With a sufficiently high fluid velocity the particles are suspended by the fluid and the whole bed of particles becomes mobile. A current feeder is installed in the bed; this can be positioned so that the current lines are either perpendicular or parallel to the electrolyte flow. This electrolyser has the advantages of fixed particulate (packed bed) electrodes (large specific area, better mass transport due to the forced flow of the electrolyte), but in addition the particles are mobile. Therefore, the material may be easily added to or taken from the cell and metal deposition does not necessarily cause difficulties with clogging of the electrode. This allows the total electrolysis current to be considerably increased. However, in addition to the potential distribution in the solution that characterizes all porous electrodes, the loss of equipotentiality of the conducting matrix due to the moving metallic particles penalizes this type of electrode. The potential transients due to the intermittent contacts between the particles and between the particles and the current feeder, affect the electrochemical reactions that take place on the surface of the particles and, therefore, the global performance of the electrolyser. It is not satisfactorily established yet how the current is transferred to the individual particles. For the particles to act as unipolar rather than bipolar electrodes, electrons must be transferred from one particle to another by electronic conduction, being generated or discharged by the appropriate electrode reaction at the surface of one particle only.

Many investigations [12] of the steady-state behaviour (current–voltage curves, potential distribution diagrams) have been carried out and have validated the model of porous electrodes proposed by Newman and Tobias [13]. This approach considers the fluidized bed electrode as a system of two pseudo-continuous phases characterized by different conductivities. In addition, the global behaviour of the fluidized bed electrode is assumed to be similar to that of a one dimensional reactor. All the studies show the important influence of the electronic conduction of the dis-

0021-891X/92

persed phases on the potential distribution in the bulk of the bed. The conduction process, which is influenced by the heterogeneous character of the fluidization and the expansion rate, is not yet understood. Various authors have proposed different modes of conduction of the electric current through the dispersed phase of the fluidized bed. The essential mechanisms are:

(i) *Convective mechanism*: the particles in their random movement in the bed undergo double layer charging when they collide with the current feeder. Then they either transmit their charge to other particles during inter-particle collisions, or discharge by faradaic reaction in the electrolyte.

(ii) *Conductive mechanism*: the conduction of current is carried out by the random formation of chains of particles that transmit the potential of the current feeder to the various regions of the bed.

(iii) *Bipolar mechanism*: the conduction of current occurs in the same way as in the convective mechanism through particle clusters or aggregates which move in the bed with one side anodically polarized and the opposite side cathodically polarized.

Very few dynamic analyses of the behaviour of the fluidized bed have been reported in the literature. To measure the equivalent resistivities of the metallic phase, Huh and Evans performed measurements of the impedance of the fluidized bed [14, 15]. These authors did not find any appreciable change in the impedance against frequency and noted the considerable influence of the bed expansion on the resistivity. Some investigations concerning fluctuations of the solution potential, of the metallic phase potential, and of the electrode overvoltage were reported [15].

In this paper a model of the fluidized bed in the dynamic regime is presented. It is based on the porous electrode model of Newman and Tobias [13] which has been tested only in steady-state situations in the case of the fluidized bed electrode. This model of a random time-varying porous electrode is described in terms of impedance in this paper and in terms of potential fluctuations in a companion paper [16].

To eliminate all the problems related to the mass change of the particles related to any deposit or dissolution process, a simple redox system was chosen: gold in NaOH solution.

2. Model

The macroscopic approach of Newman and Tobias [13] does not take into account the geometric details of the pores. The metallic conducting matrix and the electrolytic solution that surrounds the particles are considered as two continuous phases. The concentration, the current density and the potentials are average values over a volume that is sufficiently large compared with the pore structure, but sufficiently small compared to the regions where appreciable variations of these quantities are observed. This approach can be used in the modelling of a particulate bed in the fluidized regime. The measured electrical quantities can be considered as time-varying values on which random fluctuations, due to intermittent contacts between the particles, are superimposed. Therefore each quantity $X(t)$ can be considered as the sum of three terms

$$X(t) = \bar{X} + \Delta X(t) + x(t) \qquad (1)$$

where $\bar{X}$ is the mean steady-state, $\Delta X(t)$ is the mean response to a sine wave perturbation and $x(t)$ is the random fluctuation with zero mean, $\langle x(t) \rangle = 0$, due to the intermittent contacts which give rise to electrochemical noise. In this paper only the term $\Delta X(t)$ is analysed.

The electrolyte and the particulate electrode are considered by Newman and Tobias [13] as two pseudo-continuous phases locally characterized by two potentials:

$$\phi_s(M, t) \quad \text{and} \quad \phi_m(M, t)$$

at each point M of the bed and time t.

Two electric currents of density $i_s(M, t)$ and $i_m(M, t)$ flow through these two phases; the first is ionic and the second is electronic.

The equation relating the faradaic current density, i, flowing through the interface between a particle and the solution and the potential difference $E = \phi_m - \phi_s$ across the interface can be written:

$$i = \sum_j f[(\phi_m, \phi_s), C_j] \qquad (2)$$

The charge balance shows that the current densities i_m and i_s are related by:

$$\operatorname{div} i_m = -\operatorname{div} i_s = ai \qquad (3)$$

where a is the specific surface of the divided electrode.

The properties of this model were investigated in a steady-state regime for simplified situations, i.e. kinetic and diffusion limiting processes. The fluidized bed was considered as a one dimensional reactor of length L, porosity ε and specific surface a which is constant along the bed. The use of a supporting electrolyte allows the ionic migration to be neglected. All the properties of the electrolyte, except the concentrations $C_j(x)$ of the electroactive species are independent on the distance x to the current feeder. The potential distribution with the distance was calculated. It shows that for a slightly expanded bed the metallic matrix has a low resistivity and behaves equipotentially: the ohmic drop occurs mainly in the solution phase. When the bed is fluidized, the contacts between the particles are intermittent and, in this situation, the average resistivity of the metallic matrix increases considerably. In addition, the potential of the solution varies considerably with the porosity. Therefore, the faradaic current density flowing between the particles and the electrolyte is highly non-uniform in the bulk of the bed. This may lead to some regions in the bed where the particles are practically inactive, or even some regions where parasitic reactions may occur on the particles.

The properties of the porous electrodes were investigated by means of impedance measurements. To inter-

pret their dynamic behaviour Park and Macdonald have proposed to describe the porous medium by a transmission line [17]. This line can be discretized, each small section dx of the equivalent circuit of the fluidized bed being described by two resistances, R_m and R_s per unit length (Ωm^{-1}), that characterize the resistivity of the metallic matrix and the solution. The interfacial phenomena between the metal and the solution are represented by an impedance Z (Ω m).

This approach has been adapted to the characteristics of the fluidized bed where the nodes of the transmission line were supposed to represent the average positions of the particles of the fluidized bed. About these average positions the particles move and collide with each other: a contact impedance Z_m, depending on the frequency, was considered between the particles to represent their intermittent contacts when the bed is fluidized. It was assumed that Ohm's law applies to the electrolyte and the metallic phases, respectively, i.e.;

$$I_s = -\frac{1}{R_s}\frac{d\phi_s}{dx} \tag{4}$$

$$I_m = -\frac{1}{Z_m}\frac{d\phi_m}{dx} \tag{5}$$

where I_s and I_m are the currents flowing through the solution and the metallic phases respectively, R_s represents the electrolyte resistivity and Z_m the impedance due to the contacts (in Ωm^{-1}). The overvoltage across the interface between a particle and the solution at a distance x is:

$$E(x) = \phi_m(x) - \phi_s(x) \tag{6}$$

The total current flowing through a cross section of the transmission line is independent of x and is equal

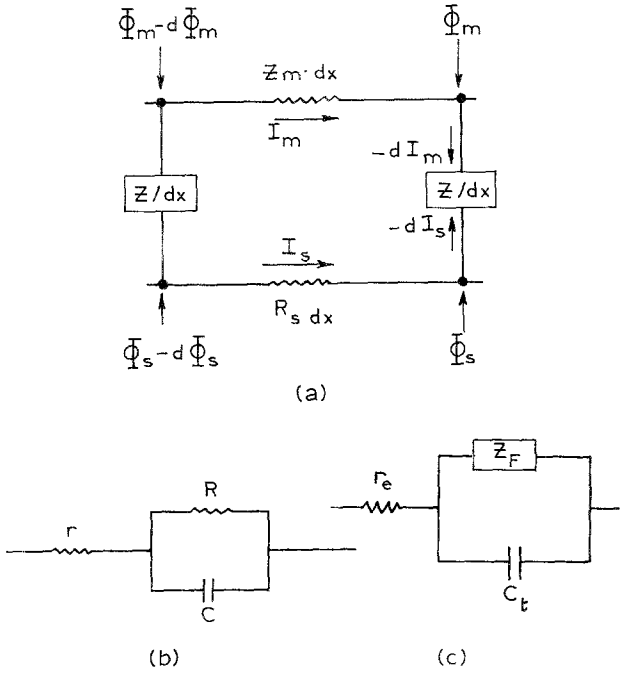

Fig. 1. Scheme of the transmission line used as a model of the fluidized bed showing: (a) elementary cell; (b) contact impedance, Z_m; and (c) interfacial impedance, Z, electrolyte resistance, r_e, faradaic impedance, Z_F, and double layer capacity, C_t.

to the electrolysis current I:

$$I = I_s(x) + I_m(x) \tag{7}$$

Differentiation of Equation 7 leads to

$$\frac{dI_s(x)}{dx} = -\frac{dI_m(x)}{dx} \tag{8}$$

and thus

$$E = -Z\frac{dI_m}{dx} = Z\frac{dI_s}{dx} \tag{9}$$

Combining Equations 4 and 9, the general equations governing the behaviour of the line schematized in Fig. 1(a) are:

$$\frac{d^2I_m}{dx^2} + \frac{1}{Z}\frac{dZ}{dx}\frac{dI_m}{dx} - \gamma I_m + \frac{R_s}{Z}I = 0 \tag{10}$$

$$\frac{d^2I_s}{dx^2} + \frac{1}{Z}\frac{dZ}{dx}\frac{dI_s}{dx} - \gamma I_m + \frac{R_m}{Z}I = 0 \tag{11}$$

$$\frac{d^2E}{dx^2} - \frac{1}{Z_m}\frac{dZ_m}{dx}\frac{d\phi_m}{dx} + \frac{1}{R_s}\frac{dR_s}{dx}\frac{d\phi_s}{dx} - \gamma E = 0 \tag{12}$$

where $\gamma = (Z_m + R_s)/Z$.

In the case where the resistance R_s and the impedances Z_m and Z are x-independent, Equations 10 and 12 simplify. By using the appropriate boundary conditions, the impedance of the fluidized bed measured between the current feeder and either the reference electrode or a metallic probe was found (see Appendix). In the simplifying conditions, where the particles and the current feeder exchange electrons without a barrier ($R'_m = 0$) and where there is no reaction between the electrolyte and the current feeder ($R'_s = \infty$), the impedance between the current feeder and the reference electrode is equal to

$$Z_{RE} = R''_s + \frac{Z_m R_s}{Z_m + R_s}L + \frac{(Z_m^2 + R_s^2)\,\mathrm{ch}\,\sqrt{\gamma}L + 2Z_m R_s}{(Z_m + R_s)\sqrt{\gamma}\,\mathrm{sh}\,\sqrt{\gamma}L} \tag{13}$$

In the case where the contact impedance Z_m is equal to a resistance R_m, Equation 13 reduces to the impedance of a pore given by Park and Macdonald [17].

In the following, the contact impedance $Z_m(\omega)$ is supposed as shown in Fig. 1(b). Moreover, the total interfacial impedance $Z(\omega)$ is as in Fig. 1(c), where r_e is the electrolyte resistance for a spherical electrode, Z_F the faradaic impedance and C_t the double layer capacity.

The high frequency limit of the impedance of the transmission line is given by

$$R_{HF} = \lim_{f\to\infty} Z_{RE}(f) = R''_s + \frac{R_s r}{R_s + r}L + \frac{(R_s^2 + r^2)\,\mathrm{ch}\,L\,((R_s + r)/r_e)^{1/2} + 2rR_s}{(R_s + r)\left(\frac{R_s + r}{r_e}\right)^{1/2}\mathrm{sh}\,L\left(\frac{R_s + r}{r_e}\right)^{1/2}} \tag{14}$$

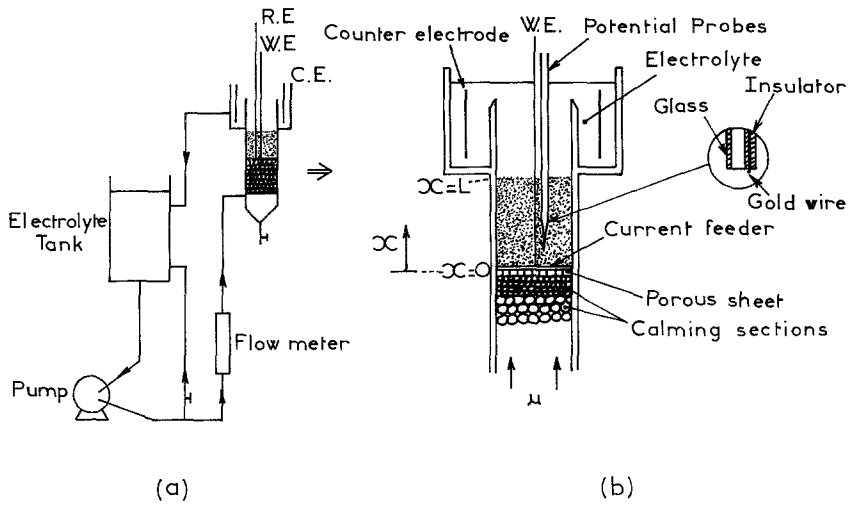

Fig. 2. Experimental arrangement used for measuring the impedance of the fluidized bed electrode in potentiostatic regime. (a) General scheme; reference electrode (R.E.); counter electrode (C.E.); working electrode (W.E.). (b) Details of the fluidized bed cell.

3. Experimental details

The fluidized bed electrolyser and its associated flow and electronic circuits are shown schematically in Fig. 2(a) and (b). The electrolyser was made of a cylindrical column 2 cm in diameter. Two compact stacks of insulating beads beneath a foil of porous polyethylene produced uniform entrance velocity. The electrolyte passed through the bed of metallized spherical particles located above a nickel grid used as the current feeder. The ensemble of the latter and of the particles constituted the divided working electrode. A nickel expanded metal grid, positioned downstream from the particulate bed, was used as a secondary electrode (counter electrode) and allowed the current to cross the bed parallel to the electrolyte flow (Fig. 2(b)).

The metallized particles were graphite spherical beads of 830 μm coated first with nickel and then with gold. Their density was 1.98 g cm^{-3}. Throughout this investigation the total mass of the particles in the bed was 5 g. The height of the packed (fixed) bed was 12 mm.

3.1. *Potential measurements*

The potentials, ϕ_m, of the metallic phase and, ϕ_s, of the electrolyte phase were measured by means of a composite probe (Fig. 2(b)). For measuring ϕ_s, this consisted of a saturated calomel reference electrode with double junction and a Luggin capillary full of the electrolytic solution. For measuring ϕ_m, it consisted of a gold wire of which the non-insulated part mimicked a motionless particle. This composite probe could be positioned in the bed at a variable distance from the current feeder by means of a micrometer screw.

3.2. *Impedance measurements*

The impedance measurements were performed by means of the experimental arrangement based on a transfer function analyser shown in Fig. 2(a). The reference electrode used was the calomel electrode of the composite probe with a Luggin capillary located 2 mm above the top of the bed. In the case of a completely fluidized bed, the very large fluctuations of the current, or of the potential, acted as a parasitic noise and dramatically perturbed the impedance measurement. In the third paper of this series this noise will be the main source of information. To obtain an impedance plot with a sufficient accuracy it is necessary to integrate the measurements over a very large number of signal periods (up to $N = 1000$ in some cases). However this technique cannot allow the low frequency domain to be explored as the measurement time becomes prohibitive.

A 1 M aqueous NaOH solution was used as the electrolyte with the gold particle fluidized bed to test the model proposed in this paper to interpret the dynamic behaviour of this electrolyser. As gold/NaOH is an ideally polarizable interface (the steady-state current is zero for any imposed potential), the bed should behave globally as a blocking electrode. Therefore it can be tested without any kinetic complication.

4. Results and discussion

4.1. *Experimental results*

Impedance measurements were carried out for various electrolyte circulation rates with the bed first packed, then close to incipient fluidization and, finally, completely fluidized (Fig. 3). The high frequency parts are given in Fig. 4. When the bed is packed but with a low electrolyte circulation rate ($u = 0.11$ cm s^{-1}) the high frequency part of the impedance diagram is a straight line with a slope slightly lower than unity (45° inclination from the real axis). For the lowest frequencies the impedance is equivalent to a straight line whose slope is close to infinity (90° inclination from the real axis). When the circulation rate increased, even without a visible bed expansion, an increase in the high frequency resistance and a capacitive loop in the very

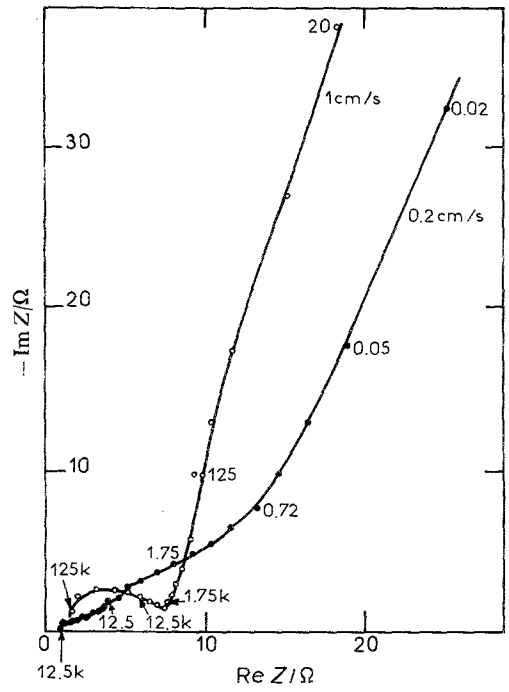

Fig. 3. Impedance of the fluidized bed electrode measured on a packed bed (fluid velocity $u = 0.2\,\mathrm{cm\,s^{-1}}$) and on a fluidized bed (fluid velocity $u = 1\,\mathrm{cm\,s^{-1}}$) of gold particles in 1 M NaOH solution. Frequencies are in hertz.

high frequency range were observed. This was equally recognizable when the bed fluidization increased. The new loop was followed by a unit slope part when the frequency decreases for intermediate circulation rate. When the bed was completely fluidized, the loop was much larger and its characteristic time-constant shifted to very high frequencies.

The impedances measured in the low frequency range for two typical regimes of the bed (fixed and fluidized) showed a dramatic increase of their magnitudes when the frequency decreases. This feature may be due either to a capacitive behaviour which is usually characteristic of a blocking electrode or to the beginning of a large loop which might be related to the relaxation of another process in the very low frequency range. Only a part of the latter would be detected as the measurement cannot be performed below 20 Hz. This limitation is due to the large fluctuations of the potential in the low frequency range related to the fluidization of the bed. The influence of an increase of the electrolyte circulation rate is shown in Fig. 5 for a bed completely fluidized. These impedance diagrams show the capacitive loop already described the characteristic frequency of which increases with the electrolyte circulation rate.

4.2. *Impedance simulation*

To discuss the experimental results, the digital simulation of the impedance predicted by the model was performed. In this first approach, only uniform transmission lines, i.e. with x-independent parameters, were studied, nonuniform transmission lines will be considered in a second paper.

The transmission line used to interpret the experimental data was based on a capacitive contact impedance Z_m such as (Fig. 1(b)):

$$Z_m = r + \frac{R}{1 + jCR\omega} \tag{15}$$

and a total interfacial impedance, Z, consisting of an electrolyte resistance, r_2, a double layer capacitance, C_2, and a faradaic interfacial impedance Z_F related to a blocking electrode (Fig. 1(c)) such as:

$$Z_F = r_1 + \frac{1}{jC_1\omega} \tag{16}$$

The elementary section of the transmission line used in the simulation is shown in Fig. 6.

4.2.1. Fixed bed. In the case where the contact impedance Z_m is zero (particles in permanent contact

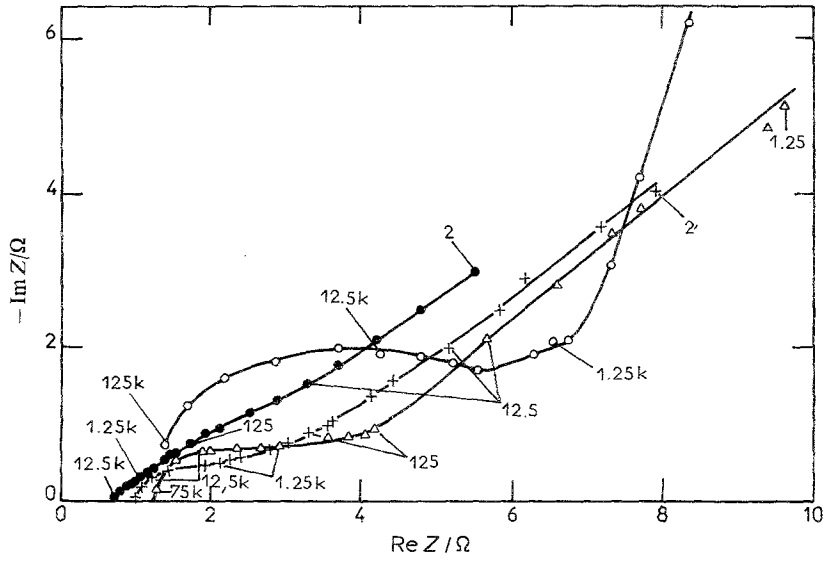

Fig. 4. High frequency part of the impedance of a fluidized bed electrode of gold particles in 1 M NaOH solution measured for various fluid velocities; packed bed for (●) $u = 0.11\,\mathrm{cm\,s^{-1}}$, (+) $u = 0.5\,\mathrm{cm\,s^{-1}}$); bed close to the incipient fluidization (△): $u = 0.5\,\mathrm{cm\,s^{-1}}$; bed totally fluidized (○): $u = 0.75\,\mathrm{cm\,s^{-1}}$. Frequencies are in hertz.

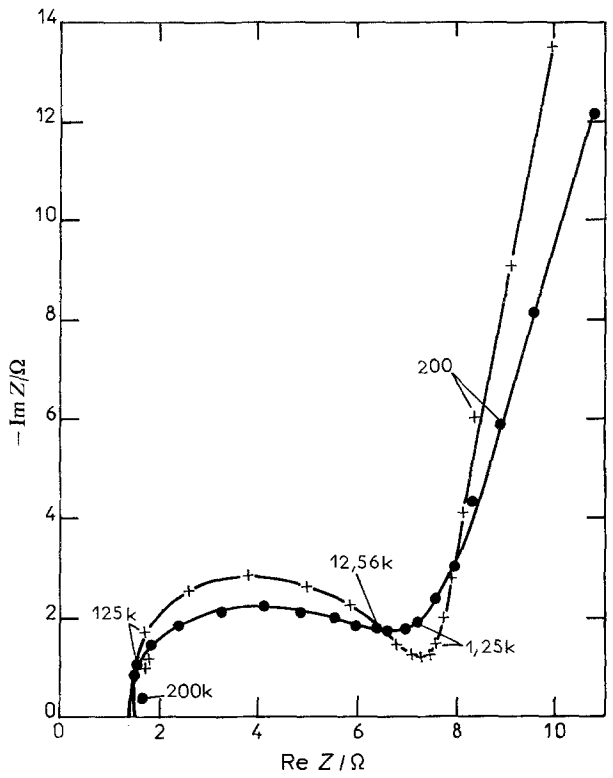

Fig. 5. Influence of the fluid velocity on the impedance of a totally fluidized gold particle bed in 1 M NaOH solution. Measurements are performed at (●) $u = 0.75\,\mathrm{cm\,s^{-1}}$ and (+) $u = 1.25\,\mathrm{cm\,s^{-1}}$ and frequencies are in hertz.

in a packed bed), a limited expansion in ω shows that in the low frequency range, the impedance is equivalent to a R_{bf}–C_{bf} series circuit, the components of which are

$$\left.\begin{aligned} R_{bf} &= \frac{L}{3}R_s + \frac{r_2}{L} + \frac{r_1 C_1^2}{(C_1 + C_2)^2 L} \\ C_{bf} &= L(C_1 + C_2) \end{aligned}\right\} \quad (17)$$

Therefore, in this case, the equivalent transmission line behaves globally as a blocking electrode.

The impedance of a fixed bed (contact impedance equal to zero) was simulated and the result is given in Fig. 7. A quasi-vertical capacitive straight line is obtained in the low frequency range and a straight line with a slope a little less than unity is observed in the medium frequency range. In the high frequency range, due to the impedance Z, the diagram approaches the real axis with a $\pi/2$ inclination.

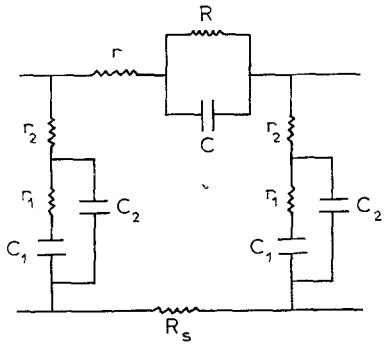

Fig. 6. Elementary cell of the transmission line used for modelling the impedance of the fluidized bed electrode.

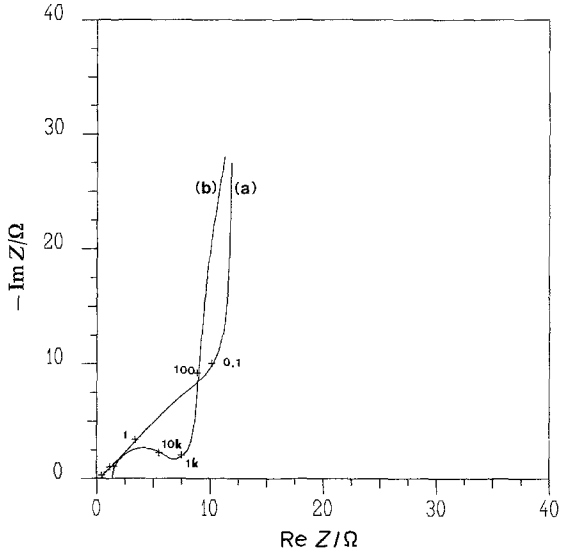

Fig. 7. Impedance of the fluidized bed calculated for (a) a packed bed and (b) a fluidized bed, for the parameters' values given in Table 1. Frequencies are in hertz.

To find a possible explanation for the intermediate slope experimentally observed (70° inclination from the real axis) in the low frequency range, a simulation of the total impedance of the bed was carried out. It was assumed that the length L of the transmission lines was not uniform over the cross section of the bed and that L was distributed following a gaussian log-normal law such as

$$p(y) = (2\pi\sigma)^{-1/2} \exp\left[-\frac{(y - \bar{y})}{2\sigma^2}\right] \quad (18)$$

where $L = \exp y$, σ is the variance and $\bar{y}$ the mean of y.

This hypothesis was tested in the simplest case, obtained from Equation 13 with $Z_m = 0$ (fixed bed) where the elementary impedance of a transmission line Z_l of length L is equal to

$$Z_l = R_s'' + (R_s Z)^{1/2} \coth\left(\frac{R_s}{Z}\right)^{1/2} L \quad (19)$$

The observed impedance, which is obtained by considering the elementary impedances in parallel, is then

$$Z(\omega)^{-1} = \int_L \frac{p(L)}{Z(\omega, L)}\,\mathrm{d}L \quad (20)$$

The simulated results are given in Fig. 8 for various variance values of the gaussian distribution of the transmission line length. A tilt of the low frequency branch is observed; this demonstrates that the similar behaviour experimentally observed could be related to the nonuniform distribution of the parameters of the transmission line over the cross section of the bed. It was shown that the nonuniform distribution of the resistivity of the solution R_s may lead to a similar behaviour where both the vertical and the 45° parts are tilted [18].

4.2.2. Fluidized bed. The impedance calculated in the case of a fluidized bed is given in Fig. 9. The values of

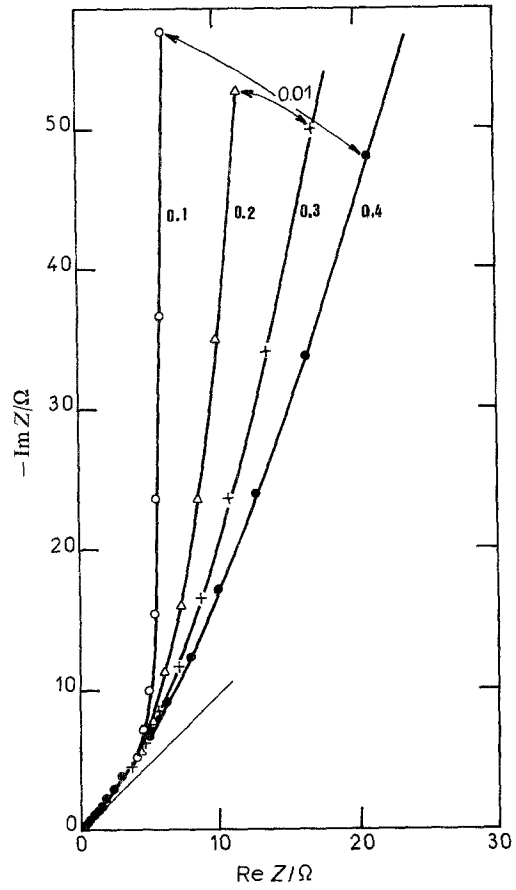

Fig. 8. Influence of a log-normal distribution of the length of the elementary transmission line on the impedance of the fluidized bed calculated for various variances. Frequency is in hertz.

the parameters that characterize the elementary section of the discretized line are listed in Table 1. The influence of the fluid circulation rate is shown in Fig. 10.

This simulation shows that concerning the very low frequency feature observed for $u = 0.2\,\mathrm{cm\,s^{-1}}$ in Fig. 3, the capacitive behaviour obtained down to 0.02 Hz on the fixed bed is actually due to the blocking property of the gold electrode in the 1 M NaOH aqueous medium. However, the low frequency increase (down to 20 Hz) observed in the case of the fluidized bed for $u = 1\,\mathrm{cm\,s^{-1}}$ in Fig. 3 seems rather to be

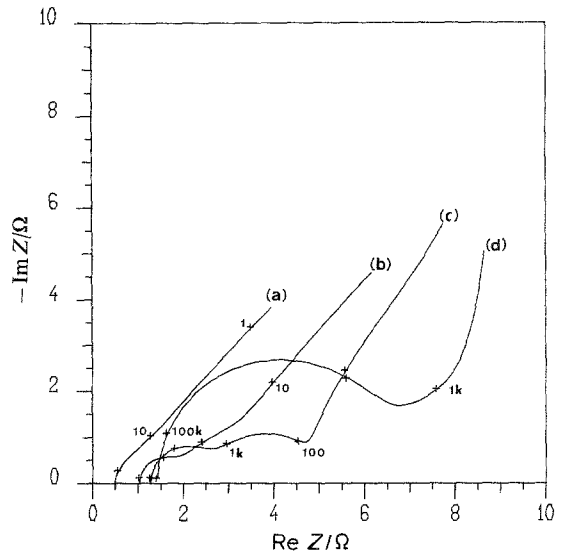

Fig. 9. Impedance of the fluidized bed calculated for the parameters values listed in Table 1. (a) Packed bed, (b) bed just before the incipient fluidization, (c) bed just after the incipient fluidization and (d) fully fluidized bed.

related to a very large capacitive loop, between 100 Hz and 1 Hz, of a kinetic origin due to the dramatic increase of the series resistance in the interfacial impedance Z circuit related to the fluidization of the bed. This capacitive loop precedes (when frequency decreases) the capacitive increase related to the blocking property of the gold/NaOH interface (see Fig. 11). If the measurements were possible to perform this low frequency capacitive increase would be found in a very much lower frequency range as the impedance measured in the 125 kHz–20 Hz range is only observable in the left lower part of the calculated diagram in Fig. 11.

The digital simulation shows that the appearance of a capacitive loop in the high frequency range is related to the circuit (r, R, C) (see Fig. 1(b)) which mimics the contact impedance between the particles. It was checked that, without this capacity C, the high frequency capacitive loop does not appear in the calculated impedance. This contact impedance is related to a time average value taken over all the intermittent contacts between the particles. The instantaneous con-

Table 1. Parameters used in the digital simulation of the impedance of the fluidized bed electrode

Parameters	*Figures*				
	7(a), 9(a)	*9(b)*	*9(c)*	*7(b), 9(d), 10(a)*	*10(b)*
$v/\mathrm{cm\,s^{-1}}$	0.11	0.5	0.5	0.75	1.25
ϕ/cm	1.2	1.2	1.2	1.3	1.6
$r_1/\Omega\,\mathrm{cm}$	0.36	0.6	0.6	410	1300
$C_2/\mathrm{F\,cm^{-1}}$	0.15	0.015	1.25×10^{-3}	1.38×10^{-4}	7.5×10^{-5}
$r_2/\Omega\,\mathrm{cm}$	8×10^{-3}	1.6×10^{-2}	3.2×10^{-2}	5.6×10^{-2}	8×10^{-2}
$R/\Omega\,\mathrm{cm^{-1}}$	0	0.75	1.25	5.8	7.5
$C/\mathrm{F\,cm}$	–	1.6×10^{-4}	1.6×10^{-5}	1.7×10^{-6}	1.1×10^{-6}
$r/\Omega\,\mathrm{cm^{-1}}$	0	0.375	0.425	0.46	0.47
$R_s/\Omega\,\mathrm{cm^{-1}}$	30	22.5	20	14	7.5
$C_1/\mathrm{F\,cm^{-1}}$	5×10^{-2}	1.25×10^{-2}	5×10^{-3}	4.6×10^{-3}	3×10^{-4}

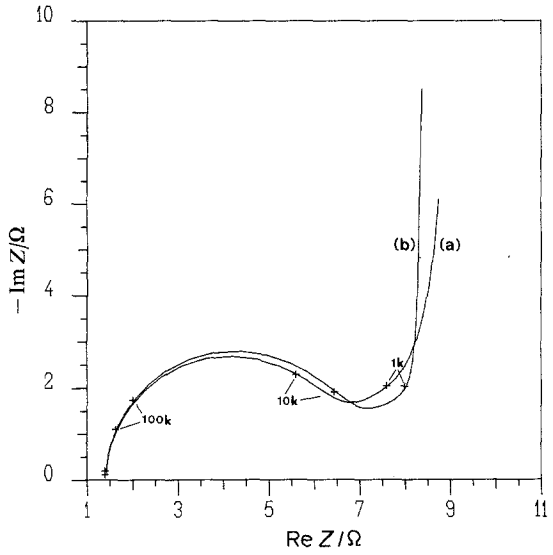

Fig. 10. Impedance of the fully fluidized bed calculated for two values of the fluid velocity. (Parameter values listed in Table 1.)

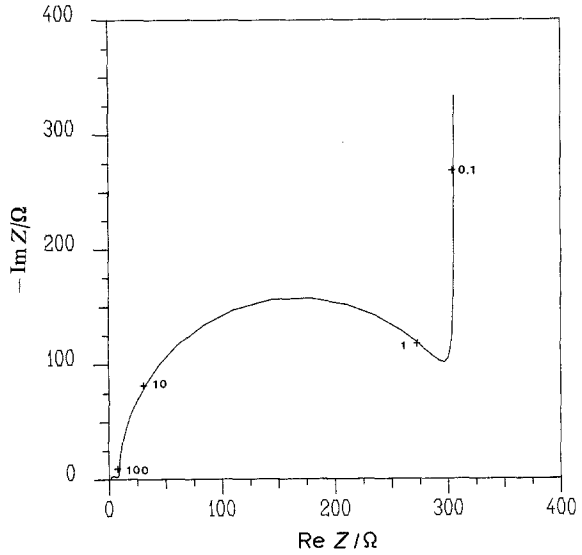

Fig. 11. Impedance of the fully fluidized bed calculated in the large frequency range with same conditions as in Fig. 7(b).

tact impedance can be supposed to be a series circuit composed of one *RC* parallel circuit related to the particle/solution interface where C is, or is related to, the double layer capacity of the first particle, one time-varying electrode resistance $r_e(t)$ between the two particles which is a function of the time-varying distance between the particles and at last another *RC* parallel circuit similar to the first one related to the second particle. When the particles collide $r_e(t)$ reaches a minimum [16].

It is necessary to note that this capacitive loop begins to appear even for relatively small fluid circulation rate when the bed appears fixed for the observer. From there, it seems that the particles of the bed imperceptibly vibrate, which break the contact during short instants between the particles sedimented at the bottom of the bed. This behaviour, largely amplified when the bed is fully fluidized, shows that the contact impedance is capacitive. When the bed is completely packed, for a very small electrolyte circulation rate, this capacitive loop disappears and only the impedance close to a 45° straight line characteristic of a potential distributed system is observed.

The digital simulation shows (see Table 1) that when the fluid circulation rate increases, the resistivity of the solution decreases; this is due to the disentanglement of the current lines that enhances the porosity, when the particles move away from one another. On the other hand, when u increases the resistances r and R increase and the capacity C decreases which is related to an increase of the contact impedance. At last, concerning the interfacial impedance the resistances r_2 and r_1 increase and the capacities C_2 and C_1 decrease when u increases. This is because for low fluid circulation rate the interfacial impedance of the gold/NaOH interface is short-circuited by the particle contacts. For higher fluid circulation rate, the number of intermittent contacts is lower and this leads to an increase of the resistances towards their values observed when the surface is free.

In conclusion, the model presented in this paper is in good agreement with the experimental results obtained in non-steady state situations. The impedance analysis of the fluidized bed electrode allows the elementary phenomena that are involved in the bed behaviour to be characterized in the case of an electroinactive process. The contact impedance between the particles, the interfacial impedance of the particle/solution interface and the solution resistivity can be determined. An application to an electroactive bed will be given in a subsequent paper [16].

References

[1] F. Coeuret, P. Le Goff and F. Vergnes, French Patent No. 1 500 269 (1967).
[2] J. R. Backhurst, M. Fleischmann, P. Goodridge and R. E. Plimley, British Patent No. 1 194 181 (1970).
[3] K. A. Spring and J. W. Evans, *J. Appl. Electrochem.* **15** (1985) 609.
[4] F. Goodridge and A. R. Wright, in 'Comprehensive Treatise of Electrochemistry', Vol. 6 (edited by E. Yeager, J. O'M. Bockris, B. E. Conway and S. Sarangapani), Plenum Press, New York (1983) p. 393.
[5] G. Van der Heiden, C. M. S. Raats and H. F. Boon, *Chem. Ind.* (July, 1978) p. 465.
[6] F. Coeuret, *Electrochim. Acta* **21** (1976) 203.
[7] G. Valentin and A. Storck, *J. Chim. Phys.* **85** (1988) 281.
[8] M. Fleischmann and J. W. Oldfield, *J. Electroanal. Chem.* **29** (1971) 231.
[9] F. Goodridge, D. I. Holden, H. D. Murray and R. E. Plimley, *Trans. Inst. Chem. Eng.* **49** (1971) 128.
[10] G. Kreysa, *Electrochim. Acta* **25** (1980) 813.
[11] M. Fleischmann and G. H. Kelsall, *Chem. & Ind.* **19** (1975) 329.
[12] B. J. Sabacky and J. W. Evans, *J. Electrochem. Soc.* **126** (1979) 1176.
[13] J. S. Newman and C. W. Tobias, *ibid.* **109** (1962) 1183.
[14] T. Huh and J. W. Evans, *J. Electrochem. Soc.* **134** (1987) 308.
[15] *Idem, ibid.* **134** (1987) 317.
[16] C. Gabrielli, F. Huet, A. Sahar and G. Valentin, to be published.
[17] J. R. Park and D. D. Macdonald, *Corros. Sci.* **23** (1983) 295.
[18] C. Gabrielli, O. Haas, F. Huet and A. Tsukada, *J. Electroanal. Chem.* **302** (1991) 59.

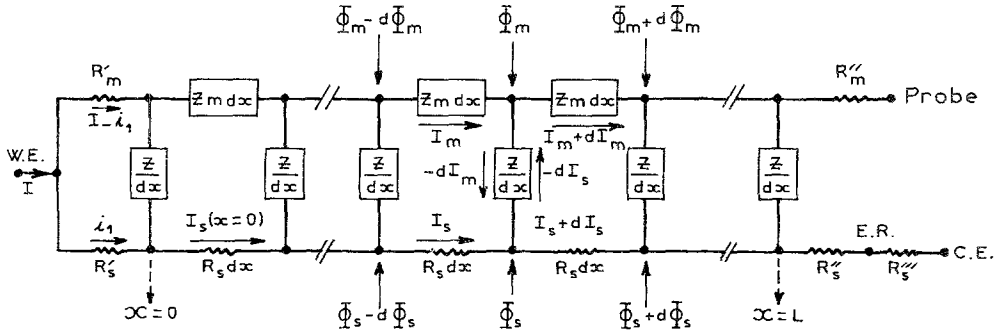

Fig. 12. Full scheme of the transmission line used for modelling the fluidized bed electrode.

Appendix

The derivation of the longitudinal impedance of the transmission line depicted in Fig. 12 which represents the fluidized bed electrode is carried out by solving the following system of equations obtained from Equations 14–16:

$$\begin{cases} \dfrac{d^2 I_m}{dx^2} - \gamma I_m + \dfrac{R_s}{Z} I = 0 \\ \dfrac{d^2 I_s}{dx^2} - \gamma I_s + \dfrac{Z_m}{Z} I = 0 \\ \dfrac{d^2 E}{dx^2} - \gamma E = 0 \end{cases} \qquad \text{(A-1)}$$

where $\gamma = (Z_m + R_s)/Z$ and the following boundary conditions apply:

$$I_m = I - i_l; \quad I_s = i_l;$$
$$E = -R'_m(I - i_l) + R'_s i_l \quad \text{for } x = 0$$
$$I_m = 0; \quad I_s = I \quad \text{for } x = L$$

where i_l and I are defined in Fig. 12.

From there, the current I_m is given by

$$I_m = C_1 \exp(-\sqrt{\gamma}x) + C_2 \exp(\sqrt{\gamma}x) + \frac{R_s I}{Z\gamma} \qquad \text{(A-2)}$$

where

$$C_1 = \frac{-i_l + \dfrac{Z_m I}{Z\gamma}\exp(\sqrt{\gamma}L) + \dfrac{R_s I}{Z\gamma}}{2 \operatorname{sh}(\sqrt{\gamma}L)}$$

and

$$C_2 = \frac{\left(-\dfrac{Z_m I}{Z\gamma} + i_l\right)\exp(-\sqrt{\gamma}L) - \dfrac{R_s I}{Z\gamma}}{2 \operatorname{sh}(\sqrt{\gamma}L)} \qquad \text{(A-3)}$$

and the overvoltage $E = \phi_m - \phi_s$ is equal to

$$E = -Z\frac{dI_m}{dx} = ZC_1\sqrt{\gamma}\exp(-\sqrt{\gamma}x) - ZC_2\sqrt{\gamma}\exp(\sqrt{\gamma}x) \qquad \text{(A-4)}$$

By using the boundary condition in $x = 0$ in Equation A-4

$$E(0) = ZC_1\sqrt{\gamma} - ZC_2\sqrt{\gamma} = -R'_m I + (R'_m + R'_s)i_l \qquad \text{(A-5)}$$

the current i_l can be determined:

$$i_l = \frac{Z_m \operatorname{ch}\sqrt{\gamma}L + R_s + R'_m\sqrt{\gamma}\operatorname{sh}(\sqrt{\gamma}L)}{(R'_m + R'_s)\operatorname{sh}(\sqrt{\gamma}L) + Z\sqrt{\gamma}\operatorname{ch}(\sqrt{\gamma}L)}\frac{I}{\sqrt{\gamma}} \qquad \text{(A-6)}$$

where $\delta = (Z_m + R_s)/Z'$ and $Z' = R'_m + R'_s$. In other words:

$$i_l = \frac{I}{Z'}\frac{Z_m \operatorname{ch}(\sqrt{\gamma}L) + R_s + R'_m\sqrt{\gamma}\operatorname{sh}(\sqrt{\gamma}L) + R_s}{\delta \operatorname{ch}(\sqrt{\gamma}L) + \sqrt{\gamma}\operatorname{sh}(\sqrt{\gamma}L)} \qquad \text{(A-7)}$$

When $R'_m = 0$, the result given in [16] is found again.

The value of the longitudinal impedance is obtained by calculating the potential drop along the line:

$$Z_l I = V_{W.E.} - V_{R.E.} = R'_m(I - i_l) + \int_0^L Z_m I_m(x)\,dx + E(x = L) + R''_0 I \qquad \text{(A-8)}$$

where $V_{W.E.}$ and $V_{R.E.}$ are respectively the potentials of the working and the reference electrodes. This leads to

$$Z_l = R''_s + \frac{Z_m R_s L}{Z_m + R_s} + \frac{2R_s\sqrt{\gamma}(Z_m R'_s - R_s R'_m) + \sqrt{\gamma}\operatorname{ch}(\sqrt{\gamma}L)[R'_s(R_s^2 + Z_m^2) + 2R_s^2 R'_m] + (Z_m + R_s)\operatorname{sh}(\sqrt{\gamma}L)[R'_s R'_m\gamma + R_s^2]}{(Z_m + R_s)\sqrt{\gamma}[(Z_m + R_s)\operatorname{ch}(\sqrt{\gamma}L) + \operatorname{sh}(\sqrt{\gamma}L)(R'_m + R'_s)]} \qquad \text{(A-9)}$$

In the limiting cases where R'_s becomes very large and R'_m tends to zero. That is,

$$\delta' \to 0 \quad \text{and} \quad Z' \to \infty$$

The expression for the impedance used to carry out the digital simulation is

$$Z_l = R''_s + \frac{Z_m R_s L}{Z_m + R_s} + \frac{(Z_m^2 + R_s^2)\operatorname{ch}(\sqrt{\gamma}L) + 2R_s R_m}{(Z_m + R_s)\sqrt{\gamma}\operatorname{sh}\sqrt{\gamma}L} \qquad \text{(A-10)}$$